PHYSICAL REVIEW E **67**, 025201(R) (2003)

Non-Gaussian random-matrix ensembles with banded spectra

Saugata Ghosh, Akhilesh Pandey, Sanjay Puri, and Rajdeep Saha
School of Physical Sciences, Jawaharlal Nehru University, New Delhi 110067, India
(Received 13 June 2002; published 10 February 2003)

Non-Gaussian random-matrix ensembles are important in many applications. We propose Monte Carlo and Langevin methods for generating non-Gaussian ensembles and their eigenvalue spectra. We also provide a general framework for analytic studies of the level density in these ensembles. We show that, in general, the level densities exhibit banded spectra, with important implications for mesoscopic systems and complex nuclei. The universality of energy-level fluctuations is confirmed.

DOI: 10.1103/PhysRevE.67.025201 PACS number(s): 05.45.Mt, 05.10.−a, 24.60.Lz

Random matrices arise in diverse physical systems [1–6], e.g., quantum chaotic systems, complex nuclei, atoms and molecules, disordered and mesoscopic systems, etc. They also occur in field-theoretic formulations of problems in condensed matter and high-energy physics [5,6].

To date, research interest has focused mainly on Gaussian random-matrix ensembles. However, recent studies indicate the relevance of non-Gaussian random-matrix ensembles in various physical applications. These ensembles were originally introduced by Dyson [7] for studies of level densities in complex many-body systems, and have recently proved useful in establishing the universality of energy-level correlations [8,9] observed in numerous examples of quantum chaotic systems. They also arise naturally in various other contexts, e.g., planar approximations in quantum field theory [5,10], models of structural glasses [11], and quantum transport problems [6].

This paper studies non-Gaussian ensembles and has two major goals. First, we propose different techniques based on Monte Carlo (MC) and Langevin dynamics to simulate these ensembles. Numerical studies of non-Gaussian ensembles have not been possible so far due to the complicated correlations (absent in Gaussian ensembles) between matrix elements. Second, we provide analytical and numerical results for energy-level spectra that exhibit multiple bands, and clearly demarcate universal and nonuniversal features. Banded spectra have received limited attention in the literature, even though we find they are generic to matrix ensembles. Such spectra have specific applications in the study of universal conductance fluctuations in mesoscopic systems, shell effects in statistical many-particle spectroscopy, and band structures in disordered solids. We elucidate some of these applications at the end of this paper.

We consider ensembles of N-dimensional matrices (H) with joint-probability density (jpd) of matrix elements given by

$$P(H) = C \exp[-\beta N \operatorname{tr} V(H)], \tag{1}$$

where C is the normalization constant. Here β labels the three standard classes of matrix ensembles, i.e., $\beta = 1,2,4$ refers to ensembles of Hermitian matrices which are real, complex, and quaternion real, respectively [1]. (The factor βN in the exponent is introduced for subsequent convenience.) The Gaussian ensembles correspond to the matrix "potential" function $V(H) = \gamma H^2/2 (\gamma > 0)$. We are interested in nonquadratic functions $V(H)$, which can give rise to banded eigenvalue spectra. Since $P(H)$ depends only on the trace of $V(H)$, the ensembles are invariant under orthogonal, unitary and symplectic transformations for $\beta = 1,2,4$ respectively. The corresponding jpd of energy levels (eigenvalues $x_1, \ldots, x_N$ of H) is [7], with c as the normalization constant,

$$p(x_1, \ldots, x_N) = c \prod_{i>j} |x_i - x_j|^{\beta} \exp\left[-\beta N \sum_k V(x_k) \right]. \tag{2}$$

This can be interpreted as a Boltzmann distribution $e^{-\beta W}$, where the "potential" W consists of a repulsive two-dimensional Coulomb (logarithmic) potential, and a one-body binding potential V.

Following Dyson, the jpd in Eqs. (1) and (2) are obtained as equilibrium ($\tau \to \infty$) densities for the following Langevin equations [7,12]:

$$\frac{dH_{jk}^{(\theta)}}{d\tau} = -\frac{\partial [N \operatorname{tr} V(H)]}{\partial H_{jk}^{(\theta)}} + \xi_{jk}^{(\theta)}(\tau), \tag{3}$$

$$\frac{dx_j}{d\tau} = \sum_{k(\neq j)} \frac{1}{x_j - x_k} - \frac{\partial [N V(x_j)]}{\partial x_j} + \xi_j(\tau). \tag{4}$$

In Eq. (3), $H_{jk}^{(\theta)}$ is the matrix element characterized by $\theta = 0, \ldots, \beta - 1$, the $H^{(\theta)}$ being the (real) component matrices of H, symmetric for $\theta = 0$ and antisymmetric for $\theta \neq 0$. The Gaussian white noises ξ in Eqs. (3) and (4) are uncorrelated, and have zero mean and variance $2\beta^{-1}$ [β^{-1} for off-diagonal elements in Eq. (3)]. For finite "time" τ, Eqs. (3) and (4) define other ensembles used, e.g., in the study of symmetry breaking in quantum chaotic systems [12,13].

Equation (3) provides a convenient prescription for generating matrices with an arbitrary distribution, and naturally incorporates the correlations between elements. Similarly, Eq. (4) gives an efficient method for generating eigenvalues in such ensembles, though one must carefully account for the unphysical level crossing induced by the discretization procedure. However, if one is interested in the equilibrium distributions alone, a faster method is available, viz., stochastic MC sampling [14] of the matrix space in Eq. (1) or the eigenvalue space in Eq. (2). The MC approach has extensive applications in diverse areas of physics [14]. In the context of Eq. (2), the MC method is implemented as follows. We start with x_j-variables ordered sequentially on a line. A stochastic move assigns, to a randomly chosen x_k, the value

$x_k' \in (x_{k-1}, x_{k+1})$ with a uniform probability. The move is accepted with probability $\exp(-\beta \Delta W)$, where ΔW is the change in potential W resulting from the move. An MC step (MCS) is defined as N moves, whether successful or not. Typically, a reasonable initial condition equilibrates very rapidly.

Let us first provide an analytic framework for the study of level density in such ensembles, which is defined as $\rho(x) = N^{-1} \int [\Sigma \delta(x - x_j)] p(x_1, \ldots, x_N) dx_1 \cdots dx_N$. For finite N, this can be obtained in terms of orthogonal and skew-orthogonal polynomials with $\exp[-\beta N V(x)]$ as the weight function [7–9]. For large N, $\rho(x)$ is the solution of the integral equation,

$$\int \frac{\rho(y)}{x-y} dy = V'(x), \tag{5}$$

valid for regions where $\rho(x) \neq 0$, the integral in Eq. (5) being the principal-value integral. Equation (5) is obtained from Eq. (4) by balancing repulsive and attractive forces for the level x_j in equilibrium, and is the minimization condition for the potential W. Note that a level introduced in the region where $\rho(x) = 0$ is not in equilibrium because it experiences a net attractive force. [In Eq. (5), the dependence on β, N have been factored out.] Using the method of Ref. [9], we can write $\rho(x)$ more explicitly in the three general cases of interest as follows.

Case I. [$V(x) \to \infty$ when $|x| \to \infty$],

$$\pi^2 \rho^2 = 2 \int \left[\frac{V'(x) - V'(y)}{x-y} \right] \rho(y) dy - [V'(x)]^2. \tag{6}$$

Case II. [$V(\pm 1) = \infty$],

$$\pi^2 (1-x^2) \rho^2 = 2 \int \left[\frac{(1-x^2)V'(x) - (1-y^2)V'(y)}{x-y} \right] \rho(y) dy - (1-x^2)[V'(x)]^2 + 1. \tag{7}$$

Case III. [$V(0) = \infty, V(x) \to \infty$ as $x \to \infty$],

$$\pi^2 x \rho^2 = 2 \int \left[\frac{xV'(x) - yV'(y)}{x-y} \right] \rho(y) dy - x[V'(x)]^2. \tag{8}$$

Equations (6)–(8) are valid when their right-hand sides are non-negative, $\rho(x)$ being zero elsewhere. Furthermore, when $V(x)$ is a low-order polynomial, the integral terms can be expressed in terms of the low-order moments of the level density, $M_p = \int x^p \rho(x) dx$, which can be interpreted as the order parameter for the onset of multiple bands in the spectrum.

As a simple example, consider the Gaussian case, $V(x) = \gamma x^2/2$ in Eq. (6), giving (since $M_0 = 1$) the "semicircle" result, $\pi^2 [\rho(x)]^2 = 2\gamma - \gamma^2 x^2$, valid for $|x| \leqslant (2/\gamma)^{1/2}$. Similarly, if $V(x) = O(N^{-1})$ in Eq. (7), then in the limit $N \to \infty$, $\rho(x) = \pi^{-1}(1-x^2)^{-1/2}$ for $|x| < 1$, extending thereby the Jacobi result of Refs. [8,9] to a larger class of weight functions. One can analogously obtain the Laguerre result of Refs. [8,9] and its extensions from Eq. (8).

In the above examples, the asymptotic density exhibits single bands. To demonstrate the two-band structure, we consider the quartic potential [11,15]

$$V(x) = \gamma \left(\frac{x^4}{4} - \alpha \frac{x^2}{2} \right), \quad \gamma > 0, \tag{9}$$

which has two minima for $\alpha > 0$, the depth of the wells being determined by the value of γ. Then, Eq. (6) yields

$$\pi^2 [\rho(x)]^2 = 2\gamma (M_2 - \alpha) + x^2 [2\gamma - \gamma^2 (x^2 - \alpha)^2]. \tag{10}$$

Now, if $M_2 = \alpha$, then $\rho(0) = 0$, suggesting the possibility of band splitting at $x = 0$; in fact $\rho(x)$ is then zero for $x^2 \leqslant \alpha - (2/\gamma)^{1/2}$ implying a two-band structure for $\alpha \geqslant \alpha_c \equiv (2/\gamma)^{1/2}$. To prove this, we evaluate M_2 by the polynomial method. Since M_2 does not depend on β, we consider $\beta = 2$ for which [7–9]

$$\rho(x) = \frac{1}{N} \sum_{\mu=0}^{N-1} (h_\mu)^{-1} [P_\mu(x)]^2 \exp[-2NV(x)], \tag{11}$$

where $P_\mu(x)$ are the orthogonal polynomials with normalization h_μ, i.e., $\int P_\mu(x) P_\nu(x) \exp[-2NV(x)] dx = h_\mu \delta_{\mu\nu}$. For monic polynomials (having highest coefficient unity), we have the three-term recursion relation, $xP_\mu = P_{\mu+1} + X_{\mu-1} P_{\mu-1}$, where $X_\mu = h_{\mu+1}/h_\mu$, for $\mu \geqslant 0$ and $X_{-1} = 0$. Since $\int dx [P_{\mu+1}(x) P_\mu(x) \exp\{-2NV(x)\}]' = 0$, we have

$$2\gamma N X_\mu (X_{\mu+1} + X_\mu + X_{\mu-1} - \alpha) = \mu + 1, \tag{12}$$

valid [16] for Eq. (9). It can be shown that, for large μ and N, X_μ alternates between $[\alpha \pm (\alpha^2 - 2\mu/\gamma N)^{1/2}]/2$ for $\mu \leqslant (\alpha/\alpha_c)^2 N$, while, for $\mu \geqslant (\alpha/\alpha_c)^2 N$, X_μ becomes $[\alpha + (\alpha^2 + 6\mu/\gamma N)^{1/2}]/6$, all three values being the same for $\mu = (\alpha/\alpha_c)^2 N$. Thus $M_2 = N^{-1} \Sigma_{\mu=0}^{N-1} (X_\mu + X_{\mu-1})$ is given, for $N \to \infty$, by

$$\begin{aligned} M_2 &= \alpha, \quad \alpha \geqslant \alpha_c, \\ &= (\gamma/27)[(\alpha^2 + 6\gamma^{-1})^{3/2} + 9\gamma^{-1}\alpha + \alpha^3], \quad \alpha \leqslant \alpha_c, \end{aligned} \tag{13}$$

the last result being valid for negative α also. Finally, Eqs. (10) and (13) yield, for $\alpha \geqslant \alpha_c$, the two-band density

$$\pi \rho(x) = \gamma |x| [2\gamma^{-1} - (x^2 - \alpha)^2]^{1/2}, \tag{14}$$

and, for $\alpha \leqslant \alpha_c$, the one-band density

$$\pi \rho(x) = \gamma [(1/3)\{(\alpha^2 + 6\gamma^{-1})^{1/2} - 2\alpha\} + x^2] \times [(2/3)\{(\alpha^2 + 6\gamma^{-1})^{1/2} + \alpha\} - x^2]^{1/2}. \tag{15}$$

In both cases, the density is zero when the right-hand sides are imaginary. Note that $\rho(x)$ for the one-band case is peaked at $x = 0$ for $\alpha \leqslant -(2/\gamma)^{1/2}$, and develops a minimum at $x = 0$ for $\alpha > -(2/\gamma)^{1/2}$. Generalized versions of Eq. (5) have been proposed in the context of disordered and mesoscopic systems [17,18]; we expect banded spectra to arise in these cases also.

The above approach is applicable to a variety of polynomial potentials in all three cases. The number of bands is

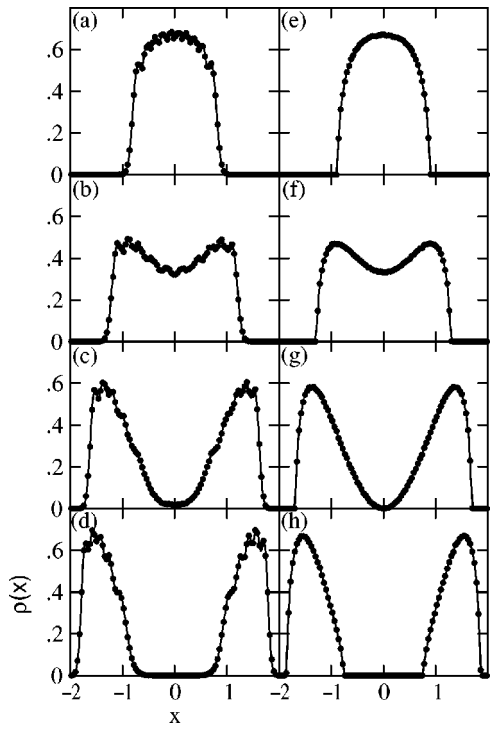

FIG. 1. Level density for the quartic potential with $\alpha=-2$, 0, $\sqrt{2}$, 2 (sequentially from the top) and $\gamma=1$. The MC results (shown as filled circles) are for $\beta=2$, and correspond to $N=10$ in (a)–(d) and $N=1000$ in (e)–(h). The solid lines are analytic results obtained from Eq. (11) in (a)–(d), and from Eqs. (14) and (15) in (e)–(h).

restricted by the number of potential minima. The only analytical difficulties arise in the evaluation of higher-order moments of the level density; however, these can be computed by numerical solution of the coefficients in the appropriate polynomial-recursion relation. We have examined several potentials in this context.

In general, multiple-well potentials (with equal depths) will lead to multiple-band spectra for sufficiently deep wells. To illustrate this, let us consider a simple potential where the number of bands (n) is a parameter:

$$V(x)=\gamma[(-1)^n\cos(n\pi x)-1], \quad |x|<1, \tag{16}$$

with hard walls at $|x|=1$ (Case II above). The parameter γ determines the depth of the potential, and, we expect an n-band spectrum for $\gamma>\gamma_c$, with the critical value depending on n.

For cases where the analytic density cannot be obtained explicitly [e.g., for the potential in Eq. (16)], one can numerically solve Eqs. (6)–(8) or compute the polynomials numerically and use Eq. (11). We have implemented a simple iterative mapping that relaxes to the equilibrium solution of Eqs. (6)–(8). However, the mapping exhibits limit-cycle behavior around bifurcation points, e.g., $\alpha=\alpha_c$ for the quartic potential. This behavior requires careful investigation. Here we present analytic results obtained using the polynomial method. The advantage of this method is that it also yields small-N density oscillations.

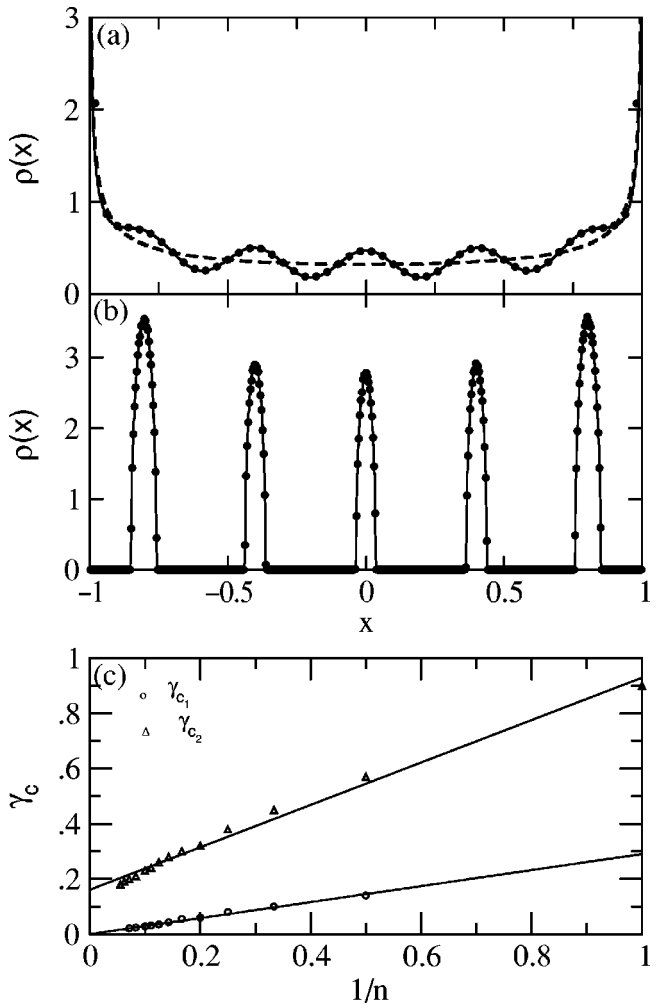

FIG. 2. Level density for the cosine potential with $n=5$ and (a) $\gamma=0.03$, (b) $\gamma=1.0$. The MC results are for $\beta=2$ and $N=1000$. Solid lines are results obtained from Eq. (11). The dashed line in (a) denotes the analytic result for $\gamma=0$, and is shown for comparison. (c) shows the polynomial results and their linear fits for γ_{c1} and γ_{c2} vs $1/n$; the fit appears to be better for γ_{c1}.

Our MC simulations were performed for a wide range of N values ($N\leqslant 1000$) with averaging over, say, $10^5/N$ spectral realizations, spaced widely apart in time (50 MCS). We have considered several potentials for $\beta=1,2,4$. We have also obtained results from the Langevin method. Here we discuss representative MC results for the quartic and cosine potentials.

For the level density $\rho(x)$, we present MC results for $\beta=2$. Figs. 1(a)–1(d) show $\rho(x)$ vs x for the quartic potential with $\gamma=1$, $N=10$, and $\alpha=-2,0,\sqrt{2},2$ demonstrating the bifurcation from the one-band case to the two-band case. We emphasize that the oscillations in the density are predicted by polynomial result (11), and a detailed examination shows that our MC method reproduces them accurately. Figures 1(e)–1(h) show analogous results for $N=1000$, which are numerically indistinguishable from analytical results (14) and (15). In fact, only about 0.01% of the numerically-obtained levels for $N=1000$ lie outside the predicted bands (which correspond to $N\to\infty$). Note that Figs. 1(b) and 1(f)

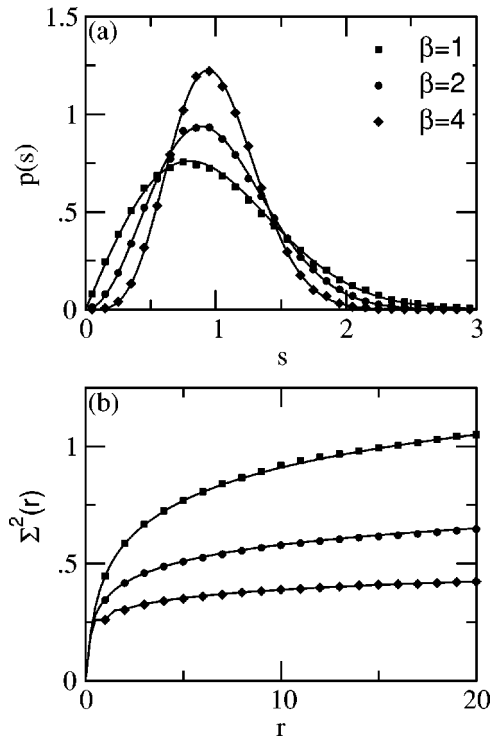

FIG. 3. (a) $p(s)$ vs s for $\beta=1,2,4$. The MC results are for the quartic potential with $\gamma=1$, $\alpha=2$ (left band), and $N=1000$. The solid lines represent the corresponding Gaussian-ensemble results [1,2], $p(s)=As^{\beta}\exp(-Bs^2)$ with A,B determined from the conditions of unit normalization and unit average spacing. (b) $\Sigma^2(r)$ vs r with MC results as in (a). The Gaussian-ensemble results are taken from [2].

correspond to the pure quartic case (i.e., $\alpha=0$). In contrast to the pure quadratic case (i.e., Gaussian ensembles), the density exhibits a dip near the origin because the attractive force for $|x|\sim 0$ is weaker in the quartic case.

Figures 2(a) and 2(b) show the MC results for the onset and formation of the multiple-band structure for the cosine potential with $n=5$ and $N=1000$. The corresponding analytic results are obtained from the polynomial method for $N\simeq 200$. We define γ_{c1} and γ_{c2} as the γ values at which the first and last band-splitting occur. The scaling dependence of these quantities on n (the number of potential minima) can be approximately ascertained by an overlap argument based on a quadratic expansion around the minima. This argument yields γ_{c1}, $\gamma_{c2}\sim 1/n$, and the polynomial results in Fig. 2(c) confirm this scaling dependence.

Next, we examine universality of the fluctuations about the level density. We have studied [1–3] (a) $p(s)$, the density of spacings s between adjacent levels and (b) $\Sigma^2(r)$, the variance of number of levels in intervals of length r, both r and s being measured in terms of the local average spacing . (The spectra were ''unfolded'' using the analytic level density.) Figures 3(a) and 3(b) show $p(s)$ and $\Sigma^2(r)$ for the quartic potential with the two-band spectra for $\alpha=2$, and $\beta=1,2,4$. Agreement with the Gaussian results is excellent, the same is also true for other values of α and other potentials. This is the first numerical confirmation of universality in non-Gaussian ensembles, and agrees with earlier predictions [8,9].

Finally, we come to specific physical applications of our results. Non-Gaussian ensembles arise in the modeling of conductance fluctuations in mesoscopic systems. Typically, these ensembles correspond to (a) different forms of $V(x)$ in Eq. (2) and/or (b) modification of the two-body interaction term [6,18]. (Similar ensembles arise in studies of the metal-insulator transition in disordered systems [17].) An important theme in mesoscopic physics is the universality of conductance fluctuations, which is a consequence of universality of *global eigenvalue correlations* in matrix ensembles. However, in the context of banded spectra, cross-band correlations are crucial, and result in the breakdown of global universality [19]. This has important physical implications, and requires detailed investigation. In a different context, the preband ing dip in the level density [cf. Figs. 1(b) and 1(f)] is analogous to shell effects in nuclear level densities, pointing to the applicability of these ensembles and their *embedded* versions to statistical many-particle spectroscopy [13].

To summarize, non-Gaussian random-matrix ensembles are of increasing importance in diverse physical applications. We have proposed different Monte Carlo and Langevin methods for generating the spectra of such ensembles. Furthermore, we have formulated an analytic framework for obtaining the level densities of these spectra. In this paper, we focused on ensembles which give rise to banded spectra. We have studied several potential functions in this context. We have confirmed the universality of energy-level fluctuations. Finally, we stress that our methods are easily adapted to ensembles of transmission and scattering matrices.

[1] M. L. Mehta, *Random Matrices* (Academic, New York, 1991).
[2] T.A. Brody *et al.*, Rev. Mod. Phys. **53**, 385 (1981).
[3] O. Bohigas and M.J. Giannoni, Lect. Notes Phys. **209**, 1 (1984).
[4] F. Haake, *Quantum Signatures Of Chaos* (Springer, Berlin, 2001).
[5] T. Guhr *et al.*, Phys. Rep. **299**, 189 (1998).
[6] C.W.J. Beenakker, Rev. Mod. Phys. **69**, 731 (1997).
[7] F.J. Dyson, J. Math. Phys. **13**, 90 (1972).
[8] A. Pandey and S. Ghosh, Phys. Rev. Lett. **87**, 024102 (2001).
[9] S. Ghosh and A. Pandey, Phys. Rev. E **65**, 046221 (2002).
[10] E. Brezin *et al.*, Commun. Math. Phys. **59**, 35 (1978).
[11] L.F. Cugliandolo *et al.*, Phys. Rev. Lett. **74**, 1012 (1995).
[12] A. Pandey, Chaos, Solitons Fractals **5**, 1275 (1995).
[13] J.B. French *et al.*, Ann. Phys. (N.Y.) **181**, 198 (1988); **181**, 235 (1988).
[14] K. Binder and D. W. Heermann, *Monte Carlo Simulation in Statistical Physics* (Springer, Berlin, 1992).
[15] E. Brezin and N. Deo, Phys. Rev. E **59**, 3901 (1999).
[16] N. Deo, J. Phys.: Condens. Matter **12**, 6629 (2000).
[17] V.E. Kravtsov and I.V. Lerner, J. Phys. A **28**, 3623 (1995).
[18] C.W.J. Beenakker and B. Rejaei, Phys. Rev. B **49**, 7499 (1994).
[19] A. Pandey and S. Puri (unpublished).